PNAS RESEARCH ARTICLE | BIOCHEMISTRY

NSUN5/TET2-directed chromatin-associated RNA modification of 5-methylcytosine to 5-hydroxymethylcytosine governs glioma immune evasion

Ruixin Wu[a,b,1], Chunming Sun[a,c,1], Xi Chen[a,1], Runyue Yang[a,d,1], Yuxuan Luan[a,e], Xiang Zhao[a], Panpan Yu[a], Rongkui Luo[f], Yingyong Hou[f], Ruotong Tian[a], Shasha Bian[a,e], Yuli Li[a], Yinghua Dong[a,g], Qian Liu[a], Weiwei Dai[a,e], Zhuoyang Fan[a], Rucheng Yan[a], Binyang Pan[a,b], Siheng Feng[a], Jing Wu[a,b], Fangzhen Chen[a,b], Changle Yang[a,b], Hanlin Wang[a], Haochen Dai[a], and Minfeng Shu[a,e,2]

Edited by Yang Shi, University of Oxford, Oxford, United Kingdom; received December 18, 2023; accepted February 28, 2024 by Editorial Board Member Peter A. Jones

Malignant glioma exhibits immune evasion characterized by highly expressing the immune checkpoint CD47. RNA 5-methylcytosine(m5C) modification plays a pivotal role in tumor pathogenesis. However, the mechanism underlying m5C-modified RNA metabolism remains unclear, as does the contribution of m5C-modified RNA to the glioma immune microenvironment. In this study, we demonstrate that the canonical 28SrRNA methyltransferase NSUN5 down-regulates β-catenin by promoting the degradation of its mRNA, leading to enhanced phagocytosis of tumor-associated macrophages (TAMs). Specifically, the NSUN5-induced suppression of β-catenin relies on its methyltransferase activity mediated by cysteine 359 (C359) and is not influenced by its localization in the nucleolus. Intriguingly, NSUN5 directly interacts with and deposits m5C on CTNNB1 caRNA (chromatin-associated RNA). NSUN5-induced recruitment of TET2 to chromatin is independent of its methyltransferase activity. The m5C modification on caRNA is subsequently oxidized into 5-hydroxymethylcytosine (5hmC) by TET2, which is dependent on its binding affinity for Fe^{2+} and α-KG. Furthermore, NSUN5 enhances the chromatin recruitment of RBFOX2 which acts as a 5hmC-specific reader to recognize and facilitate the degradation of 5hmC caRNA. Notably, hmeRIP-seq analysis reveals numerous mRNA substrates of NSUN5 that potentially undergo this mode of metabolism. In addition, NSUN5 is epigenetically suppressed by DNA methylation and is negatively correlated with IDH1-R132H mutation in glioma patients. Importantly, pharmacological blockage of DNA methylation or IDH1-R132H mutant and CD47/SIRPα signaling synergistically enhances TAM-based phagocytosis and glioma elimination in vivo. Our findings unveil a general mechanism by which NSUN5/TET2/RBFOX2 signaling regulates RNA metabolism and highlight NSUN5 targeting as a potential strategy for glioma immune therapy.

NSUN5 | RNA methylation | RBFOX2 | glioma | CTNNB1

Significance

The mechanism and fate by which the dynamic modification of m5C on RNA remain unclear. Here, we report that the canonical 28SrRNA methyltransferase NSUN5 which is epigenetically suppressed by DNA methylation is capable of introducing m5C modification on CTNNB1 caRNA. Meanwhile, NSUN5 induces chromatin recruitment of TET2 and RNA-binding protein RBFOX2. The m5C modification on caRNA is subsequently converted to 5-hydroxymethylcytosine (5hmC) by TET2, leading to its degradation through recognition by 5hmC-specific reader RBFOX2. The NSUN5/TET2/RBFOX2 signaling represents a general mechanism that controls the metabolism of m5C-modified RNA. Furthermore, NSUN5 potently blocks phagocytosis-based immune evasion via inhibiting the CD47/SIRPα pathway, suggesting that NSUN5 is a potential target for glioma immune therapy.

Over 160 types of RNA modifications have been studied, ranging from N6-methyladenosines (m6A) to pseudouridine (Ψ) (1). Among these modifications, m5C is one of the most common and significant ones (2). Members of the NSUN family act as writers of m5C with two conservative cysteine residues crucial to the methylation reaction (3). A recent study indicates that NSUN5 can stabilize target mRNA through its binding and modifying functions (4). It is reported that TET2 is involved in the modification of caRNA with 5-hydroxymethylcytosine (5hmC), leading to caRNA degradation (5). However, the mechanism by which m5C is converted to 5hmC on caRNA and 5hmC mediated caRNA metabolism remains unknown.

Malignant glioma exhibits immune evasion and is associated with a complex tumor microenvironment, with as many as 30 to 50% of cells in gliomas being tumor-associated macrophages (TAMs) (6). Rather than acting as guards or bystanders, these TAMs provide a tumor-adapted environment for glioma growth (7). The mutation of isocitrate dehydrogenase 1 and 2 (IDH1 and IDH2) is commonly found in low-grade glioma (LGG), which exhibits metabolic reprogramming and an abnormal increase in 2-HG. The excessive accumulation of 2-HG competitively inhibits dioxygenases, such as the TET family, which leads to hypermethylated CpG islands (8).

The RBFOX family of RNA-binding proteins (RBPs) has been characterized by inducing alternative splicing in a position-dependent manner (9). RBFOX1 is expressed in muscles and the brain. RBFOX3 is predominantly found in mature neurons. RBFOX2 is widely expressed in most cell types and has been reported to play a role in maintaining the correct splicing of the neural-specific splicing factor nPTB (10). Additionally, it has been shown to bind nascent RNA and inhibit transcription (11).

The authors declare no competing interest.

This article is a PNAS Direct Submission. Y.S. is a guest editor invited by the Editorial Board.

[1]R.W., C.S., X.C., and R. Yang contributed equally to this work.

[2]To whom correspondence may be addressed. Email: minfeng_shu@fudan.edu.cn.

This article contains supporting information online at https://www.pnas.org/lookup/suppl/doi:10.1073/pnas.2321611121/-/DCSupplemental.

Published March 28, 2024.

β-catenin is known to promote tumor proliferation and enable immune escape of glioma cells (12). CD47, a critical immune checkpoint (13) overexpressed in tumors, is the downstream product of β-catenin (14). CD47 is located on the surface of tumor cells and binds to the SIPRα of phagocytes, releasing a"don't eat me" signal that suppresses membrane deformation and phagocytosis of phagocytes (13). Blocking the CD47/SIRP1α axis not only increases phagocytosis around tumors but also stimulates adaptive immune reactions due to the antigen-presenting function of phagocytes, which makes it a promising therapeutic target in solid tumors, including glioma.

In our experiment, we identify that NSUN5 down-regulates β-catenin by promoting the degradation of its mRNA, resulting in enhanced phagocytosis of TAMs and glioma elimination. NSUN5 catalyzes m5C modification on CTNNB1 caRNA, which is subsequently oxidized into 5hmC by TET2. RBFOX2 as a specific reader of 5hmC, facilitating the degradation of 5hmC caRNA. The regulatory network involving NSUN5/TET2/RBFOX2 in caRNA metabolism and tumor immune microenvironment could pave the way for the development of targeted immune therapies for glioma.

Results

NSUN5 Promotes the Phagocytosis of TAMs in Glioma. Using single-cell bioinformatic analysis (*SI Appendix*, Fig. S1 *A* and *B*), we found that malignant cells exhibited the lowest NSUN5 expression levels among the different cell types that make up the tumor mass. Both in vitro (*SI Appendix*, Fig. S1 *C–J*) and in vivo experiments (*SI Appendix*, Fig. S1 *K–N*) revealed that NSUN5-overexpressed cells exhibited lower cell survival and decreased tumor migration rate, further supporting the idea that NSUN5 plays a crucial role in glioma suppression.

To investigate the specific impact of NSUN5 on the immune environment of glioma, we analyzed the infiltration of various immune cells (*SI Appendix*, Fig. S2*A*). Since macrophages comprise approximately one-third of the glioma, we sought to determine whether TAMs played a role in the regulation of NSUN5-mediated tumor growth. Surprisingly, we observed a significant inhibition of tumor growth reduction in vivo following the administration of peripheral macrophage scavenger clodronate liposomes (Fig. 1 *A–D* and *SI Appendix*, Fig. S2 *B–D*), providing insights into the function of NSUN5. Subsequently, an in vitro coculture model was established to confirm the critical role played by NSUN5 in macrophages (*SI Appendix*, Fig. S2*E*). Low-magnification microscopy revealed that tumor cells overexpressing NSUN5 were more easily engulfed, resulting in the formation of a low-pH phagolysosome (Fig. 1*E* and *SI Appendix*, Fig. S2 *F–K*). This suggests that tumor cells promote phagocytosis in an NSUN5-dependent manner. Furthermore, when CFSE-marked tumor cells were cocultured with macrophages, we observed a higher proportion of CFSE-positive macrophages in the NSUN5 overexpression group, and vice versa (Fig. 1*F* and *SI Appendix*, Fig. S2 *L* and *M*). These results suggest that NSUN5 promotes the phagocytosis of TAMs.

NSUN5 Down-Regulates CTNNB1 mRNA, Inhibiting CD47-Induced Immune Evasion of Glioma. To elucidate the mechanism by which NSUN5 promotes the phagocytosis of macrophages in the tumor immune environment, we performed mRNA sequencing

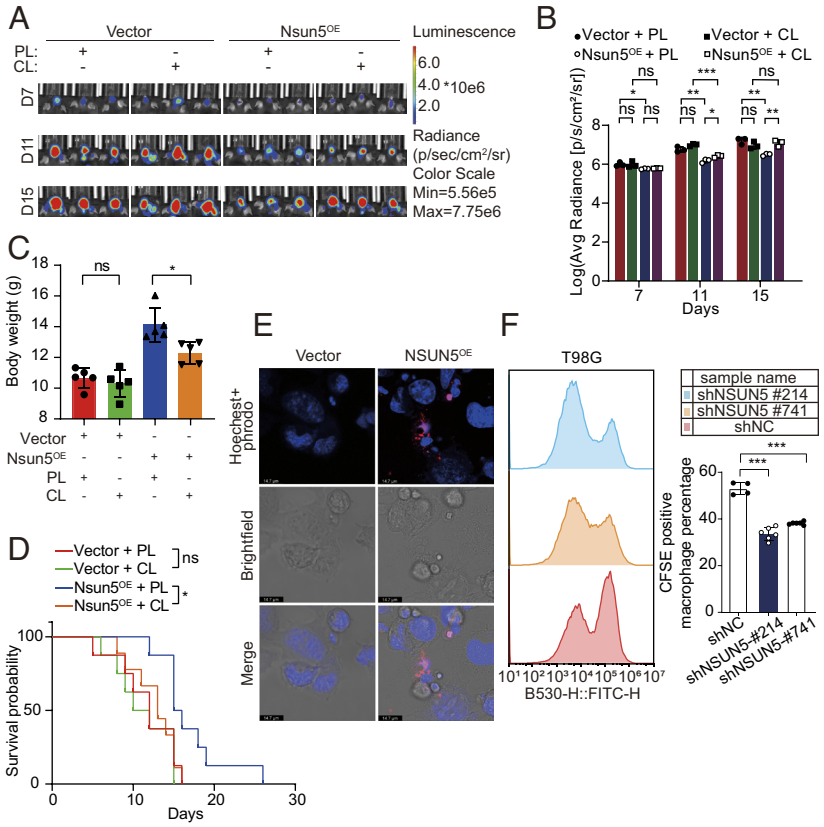

Fig. 1. NSUN5 promotes the phagocytosis of TAMs. (*A*) Representative images of the luciferase signal in C57BL/6 mice, treated with or without clodronate liposomes (CL) to eliminate macrophage;"PL" indicates PBS liposomes. (*B*) Quantification of luciferase activity in panel (*A*). (*C*) Body weight of mice on day 13. (*D*) Kaplan–Meier analysis of survival in mouse models. (*E*) Images of a coculture of GL261 and mouse peritoneal macrophages are presented, with pHrodo avidin used to label active lysosomes in red. (*F*) Flowcytometry intensity analysis of fluorescence in macrophages after phagocytosis of CFSE-labeled tumor cells in coculture experiment. The histogram shows the ratio of CFSE-positive macrophages in the coculture experiment. Data represent mean ± SD; $*P < 0.05$, $**P < 0.01$, and $***P < 0.001$.

(mRNA-seq) analysis and found that the Wnt signaling pathway was the top enriched pathway that was significantly down-regulated in NSUN5 overexpression group (Fig. 2*A* and *SI Appendix*, Fig. S3*A*). This finding aligns with the results obtained from the CGGA database (*SI Appendix*, Fig. S3*B*). CTNNB1, a key regulator of the Wnt signaling pathway was ranked first among the differentially expressed genes (Fig. 2*B*). Recently, NSUN5 is reported to methylate 28SrRNA and modulate the translation process (15). However, we observed that NSUN5 overexpression led to the downregulation of CTNNB1 and CD47 mRNA levels (Fig. 2 *C* and *D* and *SI Appendix*, Fig. S3 *C–F*), suggesting a mechanism independent of NSUN5-induced ribosome regulation. Accordingly, NSUN5 negatively regulates CTNNB1 and CD47 protein levels (Fig. 2 *E* and *F* and *SI Appendix*, Fig. S3 *G–I*). Moreover, overexpression of β-catenin or CD47 in NSUN5-transfected cells blocked the NSUN5-induced phagocytosis-enhancing effect (*SI Appendix*, Fig. S3 *J–O*).

Earlier research indicated a potential association between NSUN5 expression and genomic DNA methylation (15). Consistently, inhibiting DNMT1 through shRNA or the nonspecific inhibitor 5-Aza, which also hinders RNA methyltransferase activity (16), significantly increased NSUN5 expression (Fig. 2 *G* and *H*). Moreover, in vitro experiments combining decitabine, a specific DNMT1 inhibitor, and RRx001, a small molecular by-product from the aerospace industry (17) known to reduce CD47 and SIRPα (18), showed a notable upregulation of NSUN5 and a down-regulation of β-catenin and CD47 (Fig. 2*I*). Simultaneous administration of decitabine and RRx-001 demonstrated greater efficacy in a mouse glioma model compared to each drug alone, as evidenced by reduced tumor volume (*SI Appendix*, Fig. S3 *P–R*) and prolonged survival rates (*SI Appendix*, Fig. S3*S*). Consistently, low expression of NSUN5 and increased macrophage infiltration in the decitabine and RRx-001 combination group were observed (*SI Appendix*, Fig. S4 *A–D*). These findings suggest that disrupting the CD47-SIRPα interaction while concurrently up-regulating NSUN5 may represent a potential strategy against glioma (Fig. 2*J*).

The Suppression of β-Catenin by NSUN5 Relies on Its Methyltransferase Activity Mediated by C359 and Is Not Influenced by Its Localization in the Nucleolus. We conducted further investigations to determine whether NSUN5 regulates the expression of β-catenin through rRNA m5C modifications. Our findings indicated that overexpression of NSUN5 in multiple glioma cell lines resulted in an increase in total RNA m5C levels, whereas knockdown of NSUN5 led to a decrease in total RNA m5C levels (*SI Appendix*, Fig. S4 *E–H*), confirming its methyltransferase activity. Research has demonstrated that the cysteine residues C326 and C373 are crucial for NSUN6 methyltransferase activity. C373 performs the function of methyl transfer, while C326 releases the protein from the target RNA (19) (*SI Appendix*, Fig. S4*I*). In comparison to NSUN6, NSUN5 has two homologous cysteine residues, C308 and C359, which suggest their essential role in the methyltransferase activity of NSUN5 (*SI Appendix*, Fig. S4*J*). Intriguingly, we observed an increase in total RNA m5C modification in NSUN5-WT cells and a modest

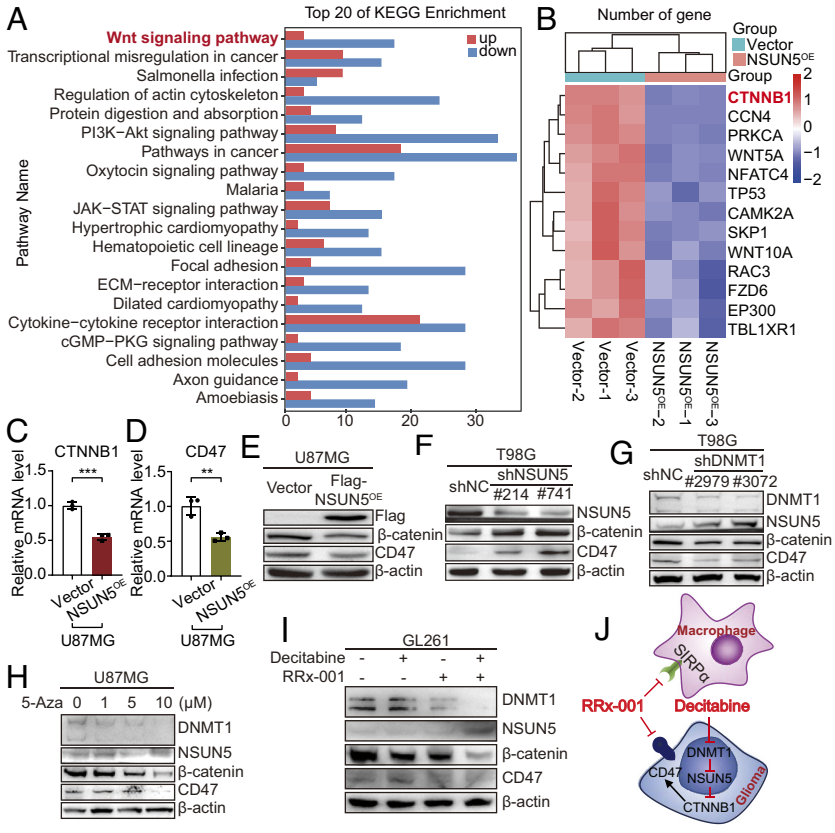

Fig. 2. NSUN5 down-regulates CTNNB1 mRNA, thereby inhibiting CD47-induced immune evasion of glioma. (*A*) The top 20 pathways with the smallest *P* values were selected for KEGG enrichment analysis. (*B*) The heatmap illustrated the genes in the Wnt signaling pathway based on our mRNA-seq results. (*C* and *D*) Relative mRNA levels of CTNNB1 and CD47, respectively. (*E* and *F*) Effect of NSUN5 on the protein levels of β-catenin and CD47 in relative cells with indicated treatments. (*G*) Effect of DNMT1 knockdown on the protein levels of NSUN5, β-catenin, and CD47. (*H*) Effect of 5-Aza treatment on the protein levels of DNMT1, NSUN5, β-catenin, and CD47. (*I*) The protein levels of DNMT1, NSUN5, β-catenin, and CD47 in GL261 cells with indicated treatments for 48 h. (*J*) A schematic diagram showing the targets of decitabine and RRx-001. Data represent mean ± SD; $^{**}P < 0.01$ and $^{***}P < 0.001$.

decrease in NSUN5-C308A cells. However, a sharp decrease was detected in NSUN5-C359A cells, suggesting a dominant negative impact on the target site by NSUN5-C359A (Fig. 3*A*). Furthermore, the downregulation of β-catenin and CD47 in cell lines containing the C359A mutation was blocked (Fig. 3*B* and *SI Appendix*, Fig. S4*K*), resulting in a decreased phagocytic capacity of TAMs surrounding cells expressing mutant NSUN5 (*SI Appendix*, Fig. S4 *L–O*). Notably, these effects were observed even in the NSUN5-C308A cell line, indicating that the NSUN5-C308A mutation may retain its methylation activity but lack recycling capability due to the covalent bond between NSUN5-C308A and mRNA.

To determine the subcellular localization of NSUN5 and where it exerts its function, an NSUN5-GR (glucocorticoid receptor of rat) fusion protein was expressed in U87MG cells and was induced to translocate to the nucleus by adding triamcinolone acetonide (TA) to the medium (20). After confirming the reliability of the method using confocal microscopy and western blotting (*SI Appendix*, Fig. S5 *A–C* and Fig. 3*C*), our analysis showed that the nuclear localization of NSUN5 enhanced its effects on suppressing β-catenin expression and inducing phagocytosis (Fig. 3 *D* and *E* and *SI Appendix*, Fig. S5 *D* and *E*).

It is reported that NSUN5 functions as a rRNA methyltransferase to modulate the translation process when resides in the nucleolus (15). To investigate whether NSUN5 regulates β-catenin expression is dependent on its nucleolus localization, we first generated an NSUN5 mutant that exclusively localizes outside of the nucleolus by deleting its 1 to 120 amino acids (21) (Fig. 3*F* and *SI Appendix*, Fig. S5*F*). The m5C modification level in 28S rRNA significantly decreased in U251MG-NSUN5△120 (Fig. 3*G*). Remarkably, NSUN5-△120 still functioned as a repressor of β-catenin expression (Fig. 3 *H* and *I* and *SI Appendix*, Fig. S5 *G* and *H*), suggesting the presence of alternative mechanisms. Next, we performed m5C dot-blot and LCMS/MS with mRNA samples purified using oligo(dT) magnetic beads. As anticipated, more m5C modifications were detected in the presence of NSUN5 or NSUN5-△120 (Fig. 4*A* and *SI Appendix*, Fig. S6 *A* and *B*).

NSUN5 Deposits m5C on CTNNB1 mRNA, Thus Promoting Its Degradation. To determine whether NSUN5 can directly bind to the mRNA of CTNNB1, an Aza-IP sequencing was carried out on two separate RNA samples, resulting in a list of 5,617 mRNAs. Among them, 1,573 genes were up-regulated and 1,891 genes were down-regulated according to mRNA-seq, including CTNNB1 which is marked in the Volcano plot representing the 3,464 genes in the intersection (Fig. 4*B* and *SI Appendix*, Fig. S6*C*). The GO enrichment analysis of the up and down-regulated genes revealed that various signal pathways related to cancers were either activated or inhibited (*SI Appendix*, Fig. S6*D*). Moreover, after removing rRNA, we observed that protein-coding RNAs accounted for 62% of the genotypes, with a significant proportion of exons, indicating the crucial role of NSUN5 in mRNA modulation (*SI Appendix*, Fig. S6 *E* and *F*). Notably, CTNNB1 was found to be significantly enriched (*SI Appendix*, Fig. S6*G*). NSUN5 overexpression significantly promoted the degradation of CTNNB1 mRNA, while knocking down endogenous NSUN5 enhanced the stability of

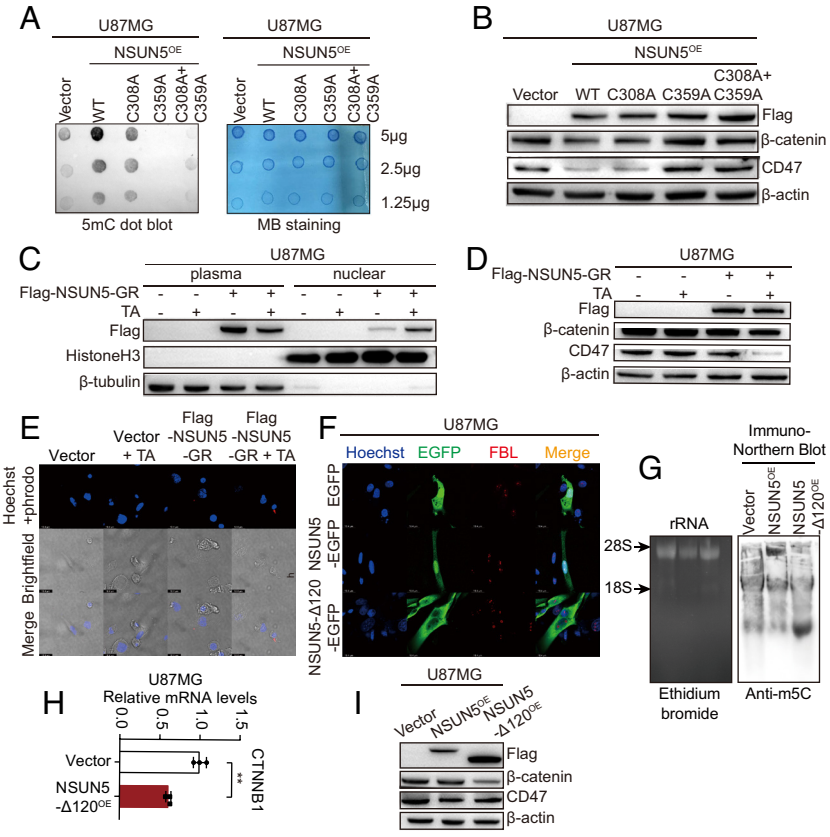

Fig. 3. The NSUN5-induced suppression of β-catenin relies on its methyltransferase activity, regardless of its localization in the nucleolus. (*A*) m5C dot blot analysis. Methylene blue (MB) staining was used as a loading control. (*B*) Effects of NSUN5 mutants on β-catenin and CD47 protein expression. (*C*) Fractionation analysis of the Flag-NSUN5-GR protein level in the plasma and nuclear components of U87MG cells treated with or without TA. Histone H3 and β-tubulin were used as the loading control for the nucleus and cytoplasm, respectively. (*D*) The protein levels of Flag-NSUN5-GR, β-catenin, and CD47 in U87MG cells. (*E*) Fluorescence images of pHrodo-stained cocultured cells. (*F*) Subcellular localization analysis in U87MG cells. FBL was used as a nucleolus marker. (*G*) Immuno-Northern blot analysis of m5C modification on 28s rRNA. (*H*) Relative CTNNB1 mRNA levels. (*I*) The protein levels of β-catenin and CD47. Data represent mean ± SD; $^{**}P < 0.01$.

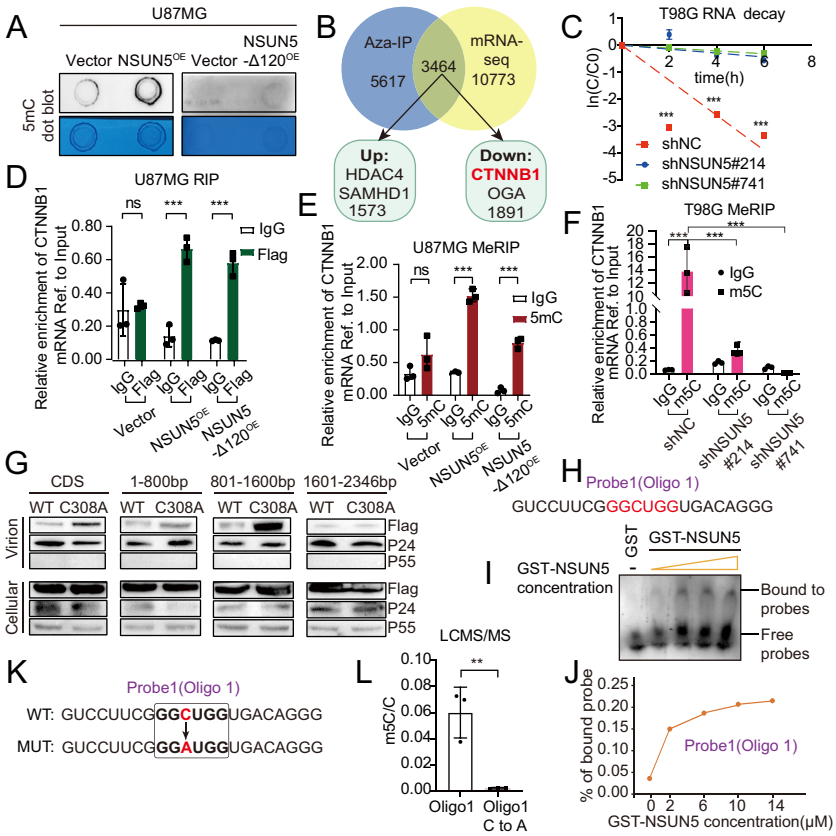

Fig. 4. NSUN5 deposits m5C on CTNNB1 mRNA, thus promoting its degradation. (*A*) m5C dot blot analysis in U87MG cells. (*B*) Analyzing the mRNA enriched in Aza-IP alongside the differentially expressed genes identified in RNA-seq revealed that 1,573 genes were up-regulated, while 1,891 genes were down-regulated. (*C*) CTNNB1 mRNA decay assay. (*D*) The enrichment of CTNNB1 mRNA immunoprecipitated by anti-Flag antibody was assessed in U87MG cells. (*E* and *F*) The enrichment of CTNNB1 mRNA immunoprecipitated by anti-m5c antibody was assessed. (*G*) The proteins contained in the supernatant and cell components were analyzed. P24, the lentivirus capsid protein, was used as an indicator of the presence of the virus. P55, the precursor of p24, was only found in cell components, indicating successful separation. (*H*) The sequence of RNA probe 1. (*I*) RNA EMSA experiments. (*J*) The percentage of probe1 bound by GST-NSUN5 was quantified. (*K*) The sequence of WT and mutant probe 1. (*L*) LCMS/MS analysis of the m5C modification on the oligos which mediated by NSUN5 through the in vitro methylation. Data represent mean ± SD; "ns" indicates not significant, $^{**}P < 0.01$, and $^{***}P < 0.001$.

CTNNB1 mRNA (Fig. 4*C* and *SI Appendix*, Fig. S6 *H* and *I*). RNA immunoprecipitation (RIP) assay revealed that both NSUN5 and NSUN5△120 can directly bind to CTNNB1 mRNA (Fig. 4*D* and *SI Appendix*, Fig. S6*J*). Furthermore, m5C-MeRIP showed that both NSUN5 and NSUN5-△120 overexpression significantly increased the m5C abundance on CTNNB1 mRNA, while knocking down endogenous NSUN5 diminished the m5C level on CTNNB1 (Fig. 4 *E* and *F* and *SI Appendix*, Fig. S6*K*), confirming that NSUN5 plays a significant role in depositing m5C modifications on CTNNB1 mRNA. These findings suggest that NSUN5-mediated m5C modification on CTNNB1 mRNA may induce its degradation.

We speculated that the 359 cystine of NSUN5-C308A mutant could covalently bind to its targeted "C." To confirm this covalent modification on the 308 cystine to alanine mutant NSUN5, we conducted RNase-LCMS/MS analysis (*SI Appendix*, Fig. S7 *A–E*). We did not find complete cytidine at 359C, but instead detected acylation at 359C, formylation at 361C, and acetylation at 310G. We speculated that the original covalently binding cytidine has been decomposed due to the acidic substances used in mass spectrum processing. Based on these pieces of evidence, we conducted a lentivirus-packaging experiment (*SI Appendix*, Fig. S8*A*) to identify the binding site on the transcript of CTNNB1 drawing on the prediction that NSUN5-C308A mutant would be packaged into lentivirus when the viral genome contains a targeted "C." Our results suggested that the middle part (801 to 1,600 bp) might be a possible binding site (Fig. 4*G*). Based on the motif predicted by Aza-IP seq analysis (*SI Appendix*, Fig. S8*B*), we designed several probes for the REMSA experiment, two of which showed dose-dependent binding capacity (*SI Appendix*, Fig. S8 *C–F* and Fig. 4 *H–J*). We also performed mutations on the methylation sites of the two probes and utilized recombinant NSUN5 to conduct in vitro methylation experiments. The results demonstrated a decrease in the level of m5C on the mutant probes (Fig. 4 *K* and *L* and *SI Appendix*, Fig. S8 *G* and *H*). Collectively, our findings show that NSUN5 can bind to the transcript of CTNNB1 and deposit m5C modifications on two potential sites, thereby promoting its degradation.

NSUN5 Catalyzes the Formation of m5C on CTNNB1 caRNAs, Which Are Subsequently Oxidized by TET2 for Further Processing. To gain a better understanding of the types of mRNA influenced by NSUN5, we isolated RNAs from cytoplasm, nucleoplasm, and chromatin (*SI Appendix*, Fig. S9*A*) and measured their proportions. Surprisingly, we observed a dramatic decrease in the proportion of CTNNB1 mRNA in the chromatin-associated RNA (caRNA) fraction in NSUN5 overexpressing U87MG cell line (Fig. 5*A*), resulting from a notably decreased half-life (Fig. 5*B*). In addition, NSUN5 overexpression exhibited little effect on non-caRNA stability (*SI Appendix*, Fig. S9 *B–D*). These findings provide further support for our conclusion that NSUN5 functions as a key regulator of CTNNB1 expression through its

role in caRNA regulation. Notably, in NSUN5 transfected cells, higher levels of 5hmc were detected in both total RNA (Fig. 5*C* and *SI Appendix*, Fig. S9 *E* and *F*) and CTNNB1 mRNA (Fig. 5 *D* and *E*). Furthermore, NSUN5-C308A, but not NSUN5-C359A mutant transfection also resulted in accumulated 5hmc in CTNNB1 mRNA (Fig. 5*F*). TET2 is a well-known DNA m5C dioxygenase (22), which can decrease the level of caRNA by converting m5C to 5hmC (5). Knockdown of either NSUN5 or TET2 mitigated the decrease in β-catenin induced by TET2 or NSUN5, respectively (Fig. 5 *G* and *H*), indicating that both are necessary to destabilize CTNNB1 mRNA.TET2 has several crucial catalytic sites, including Fe^{2+} and α-KG binding sites (essential cofactors of TET2) and a DNA-binding site (23). Our finding indicated that the wild-type (WT) TET2 expression resulted in a reduction of m5C and an increase in 5hmC levels, which was linked to its binding affinity for Fe^{2+} (ΔHxD) and α-KG (Δα-KG), but not for DNA (ΔDNA) (Fig. 5 *I* and *J* and *SI Appendix*, Fig. S9*G*). Moreover, knockdown of endogenous TET2 significantly diminished the 5hmC modification on CTNNB1 mRNA (*SI Appendix*, Fig. S9*H*). Accordingly, a decline in the levels of CTNNB1 mRNA and protein was observed only in TET2(WT) or TET2(ΔDNA) expressed cells (Fig. 5 *K* and *L*).

As nascent RNA is primarily situated on chromatin prior to undergoing additional modification and processing, it is also regarded as a form of caRNA that is potentially affected by TET2. To investigate the effect of NSUN5 on degradation of nascent RNA, we used the click reaction of 5-Ethynyluridine (EU) and found that NSUN5 resulted in a higher rate of degradation of nascent RNA (Fig. 5 *M* and *N*). It is worth noting that NSUN5 induces recruitment of TET2 from the cytoplasm to chromatin, regardless of its methyltransferase activity (Fig. 5 *O* and *P*). In addition, isolation of protein on the nascent RNA(IPONR) analysis showed a significant enrichment of TET2 in NSUN5 overexpression cells (Fig. 5*Q*). To test the hypothesis that nascent RNA of CTNNB1 catalyzed by NSUN5 is degraded in a TET2-dependent manner, the caRIP experiment was conducted, and we found that NSUN5 enhances the interaction between TET2 and CTNNB1 caRNA (Fig. 5 *R* and *S*). However, we did not find any direct interaction between NSUN5 and TET2 (*SI Appendix*, Fig. S9*I*). Nevertheless, we observed spatial colocalization of NSUN5 and paraspeckle (*SI Appendix*, Fig. S9*J*), which is a phase separation structure that mainly processes and modifies mRNA (24), suggesting that there might be alternative mechanisms involved in the recruitment of TET2. These findings indicate that TET2 acts downstream of NSUN5 to mediate the transition of m5C to 5hmC on CTNNB1 caRNA (Fig. 5*T*).

RBFOX2 Is a Potential Reader of RNA 5hmC and Mediates the Degradation of CTNNB1 caRNA. To determine which protein could recognize RNA 5hmC and mediate the degradation of CTNNB1 caRNA, recombinant TET2 protein was used to facilitate the oxidation of a probe containing m5C, and borane-ammonia was employed to reduce overoxidized forms, such as 5fC and 5caC, to 5hmC (Fig. 6*A*). The efficacy of oxidation was measured using LCMS/MS (Fig. 6*B*). Subsequently, the probe was biotin-labeled and used for RNA pull-down followed by Mass Spectrometry analysis (Dataset S3). Our findings identify RBFOX2 as a potential candidate reader capable of recognizing and binding to 5hmC RNA, rather than m5C RNA (Fig. 6*C*). We further confirmed that RBFOX2 accelerated the degradation of CTNNB1 mRNA (Fig. 6*D*) and reduced β-catenin protein levels (Fig. 6*E* and *SI Appendix*, Fig. S10*A*). In addition, knockdown of NSUN5 in RBFOX2-overexpressing glioma cells rescued the levels of β-catenin, further supporting the connection between RBFOX2-mediated degradation and NSUN5 (Fig. 6*F*). Next, recombinant RBFOX2 protein (*SI Appendix*, Fig. S10*B*) was incubated with total RNA or a 1:1 mixture of m5C oligo and 5hmC oligo as targets. In vitro RIP (iv-RIP) assays demonstrated that RNA bound by RBFOX2 contained a higher level of 5hmC (Fig. 6 *G* and *H*). Furthermore, Isolation of Proteins on Nascent RNA (IPONR) assays revealed that NSUN5 increased RBFOX2 binding to nascent RNA (Fig. 6*I*), as well as to CTNNB1 caRNA, as demonstrated by caRIP (Fig. 6*J*).

To validate the broader significance of our findings, hmeRIP-seq analysis was conducted, revealing that the enrichment of motifs ("U(C/G)CCUGG") associated with 5hmC is highly consistent with the top motif ("GCCUGG") enriched in the Aza-IP-seq (*SI Appendix*, Fig. S10*C*). Interestingly, a recent report shows that the top motif recognized by RBFOX2 is "GCCUGG," which is consistent with our findings (*SI Appendix*, Fig. S10*C*) (25). In addition, the RBFOX2 eCLIP-seq peak is consistent with the 5hmC-RIP-seq (*SI Appendix*, Fig. S10*D*). We further conducted an RNA EMSA assay to test the RBFOX2's binding affinity for hm5C-containing transcripts and found that the recombinant His-tagged RBFOX2 protein could strongly bind to hm5C oligo (*SI Appendix*, Fig. S10*E*). These data suggest that RBFOX2 acts as a reader for RNA hm5C. Among the 5564 genes enriched by hmeRIP, 612 of them were also enriched by Aza-IP and showed decreased expression in RNA-seq analysis (*SI Appendix*, Fig. S10*F*). To further confirm the functional impact of NSUN5 on these genes, we selected four of them (RAB5B, MAP2K4, SLC16A3, SOX9) and conducted RNA decay assays. The results revealed that NSUN5 induced a significantly higher rate of degradation for all four genes (*SI Appendix*, Fig. S10*G*). Our findings unveil that the NSUN5/RBFOX2 axis represents a general mechanism that regulates RNA metabolism in a 5mC/5hmC-dependent manner.

The IDH1-R132H Mutation Down-Regulates NSUN5 by Affecting Its Genomic Methylation. IDH1-R132H is a prevalent mutation in LGG. Previously, research has demonstrated that mutant IDH1 can form a heterodimer with WT form, converting α-KG into 2-HG (26), which inhibits the function of demethyltransferases and leads to a highly methylated genome. Using RNA-seq data from the CGGA database, we found a negative correlation between NSUN5 gene expression and IDH mutation status (*SI Appendix*, Fig. S11*A*). Moreover, IDH1-R132H mutation led to a decrease in NSUN5 levels (Fig. 7*A* and *SI Appendix*, Fig. S11*B*) and m5C levels in total RNA (Fig. 7*B* and *SI Appendix*, Fig. S11*C*), followed by an inhibition in TAM phagocytosis (Fig. 7*C*). The downstream genes NAPRT1 and PD-L1 were also analyzed (*SI Appendix*, Fig. S11*D*). The m5C-meDIP assay confirmed a relatively higher m5C modification on the CpG island within the NSUN5 promoter upon IDH1-R132H transfection (Fig. 7*D*). The protein levels of β-catenin (Fig. 7*E*) and TAM phagocytosis (Fig. 7*F*) were significantly restored in cells transfected with NSUN5. Additionally, IDH1-R132H has been shown to promote a suppressed tumor immune environment (27–29). We also observed a better cell survival in IDH1-R132H-transfected cells (*SI Appendix*, Fig. S11*E*). Patient samples further confirmed low expression of NSUN5 in IDH1-R132H mutant patients, as well as low macrophage infiltration (Fig. 7 *G*–*J*). Our data indicate that the IDH1-R132H mutation may impact the tumor immune microenvironment by targeting NSUN5.

RRx-001 Enhances the Antitumor Effect of Ivosidenib in IDH1 Mutant Gliomas. As demonstrated in our study, DNMT1 and IDH1-R132H can epigenetically down-regulate NSUN5, leading to the suppression of the β-catenin-CD47 signaling pathway in

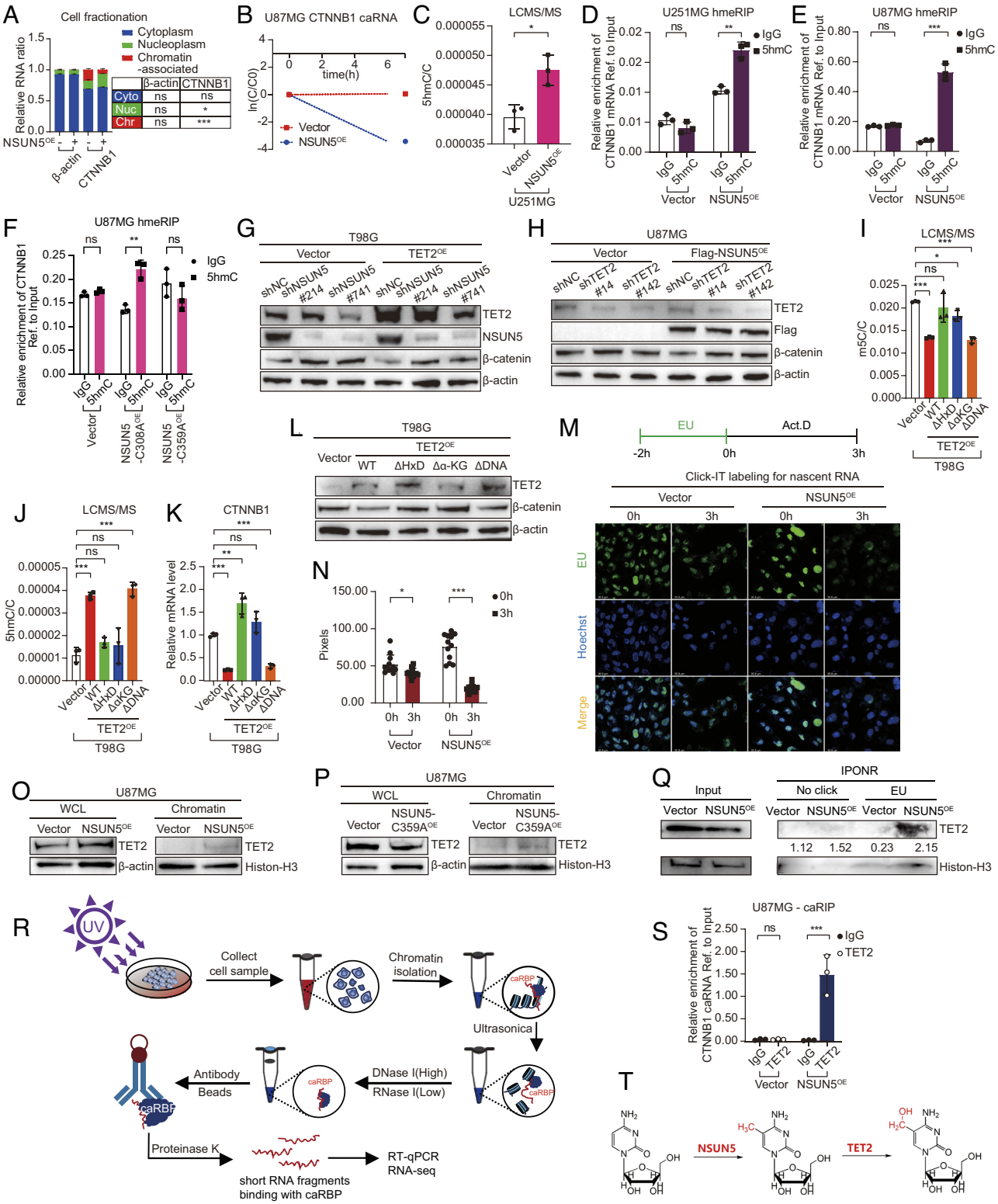

Fig. 5. NSUN5 catalyzes the formation of m5C in CTNNB1 caRNAs, which are subsequently modified by TET2 for further processing. (*A*) Quantification of CTNNB1 mRNA levels was performed by qPCR in the cytoplasm, nucleoplasm, and chromatin of U87MG cells. (*B*) The caRNA was fractionated, and qPCR was performed to measure the rate of RNA decay. (*C*) The 5hmC levels were quantified by LCMS/MS. (*D–F*) The enrichment of CTNNB1 mRNA immunoprecipitated by anti-5hmc antibody was assessed. (*G* and *H*) The β-catenin protein levels were detected. (*I* and *J*) The m5C and 5hmC levels were quantified by LCMS/MS. (*K*) Relative CTNNB1 mRNA levels. (*L*) The β-catenin protein levels were measured. (*M*) The nascent RNA metabolically labeled with EU (green) was measured in U251MG cells with indicated treatments. (*N*) The relative mean gray value of EU in the indicated cells was quantified. 12 cells were randomly chosen for analysis. (*O* and *P*) The TET2 protein levels in the whole-cell lysate (WCL) and chromatin proportion. β-actin and histone H3 served as internal references of WCL and chromatin proteins, respectively. (*Q*) Isolation of protein on the nascent RNA (IPONR) assay was conducted in U251MG cells. The TET2 protein binding to nascent RNA separated by click reaction was detected and quantified. (*R*) The experimental flow showed that chromatin-associated components were fractionated, and anti-TET2 was used to enrich its binding caRNA. (*S*) The caRNAs bound to TET2 were first immunoprecipitated with anti-TET2 antibody. The enrichment of CTNNB1 caRNA was further measured using qPCR from the TET2 immunoprecipitated caRNAs. (*T*) Schematic diagram showing the sequential formation of m5C and 5hmC induced by NSUN5 and TET2. Data represent mean ± SD; "ns" indicates not significant, **P* < 0.05, ***P* < 0.01, and ****P* < 0.001.

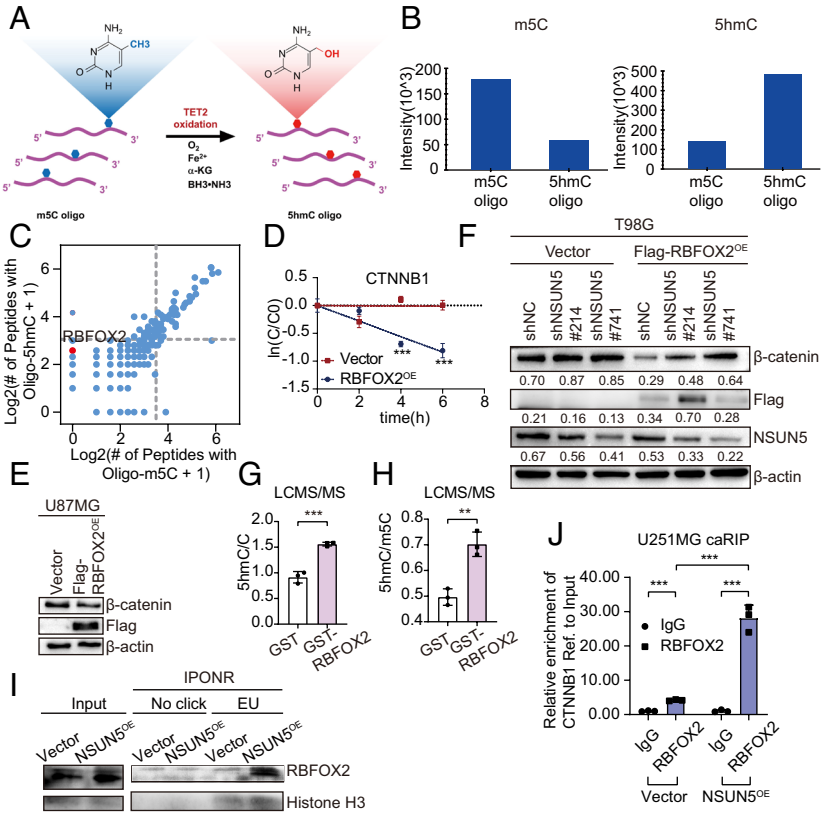

Fig. 6. RBFOX2 is a reader of RNA 5hmC and mediates the degradation of CTNNB1 caRNA. (*A*) A schematic diagram illustrating the synthesis of the 5hmC probe was generated. (*B*) The extent of m5C and 5hmC modifications on the probes was determined by mass spectrometry analysis. (*C*) A scatter plot was generated to depict the proteins bound to Oligo5hmC versus Oligo-m5C RNA oligos. The plot was based on the average peptide numbers of proteins detected in both replicates, with the enriched RBFOX2 protein highlighted. (*D*) The CTNNB1 mRNA decay assay was detected in U251MG cells. (*E*) Effect of RBFOX2 on β-catenin protein expression in U87MG cells. (*F*) β-catenin and NSUN5 protein levels were detected and quantified. (*G* and *H*) LCMS/MS analysis was conducted on the indicated RNA molecules that were enriched by RBFOX2 immunoprecipitation (iv-RIP). (*I*) An IPONR assay was performed in U251MG cells. RBFOX2 protein binding to nascent RNA separated by click reaction was detected. (*J*) The enrichment of CTNNB1 caRNA was measured using qPCR from the caRNAs immunoprecipitated with an anti-RBFOX2 antibody. Data represent mean ± SD; $^{**}P < 0.01$ and $^{***}P < 0.001$.

a TET2/RBFOX2-dependent manner and ultimately reducing TAM phagocytosis. Our in vitro experiments demonstrated that a lower dose of RRX-001 can increase the expression of NSUN5 in WT glioma cells compared to IDH1-R132H mutant glioma cells, indicating that WT gliomas are more responsive to RRX-001 treatment (Fig. 8*A*). In recent years, much attention has been given to drugs targeting mutant IDH1, with ivosidenib and olutasidenib being approved by the FDA for the treatment of acute myeloid leukemia and cholangiocarcinoma, respectively (30, 31). However, their applications in glioma are still obscure. Our findings revealed that combining ivosidenib with RRx-001 synergistically induced NSUN5 and down-regulated β-catenin and CD47, particularly in IDH1-R132H mutant glioma (Fig. 8*B*). This was consistent with a lower cell viability (Fig. 8*C*). Additionally, in situ glioma model in C57BL/6 mice confirmed our conclusion in vivo (Fig. 8 *D*–*G*). Immunofluorescence analysis of tissue slices demonstrated increased macrophage infiltration in the group treated with the combination of ivosidenib and RRx-001 (Fig. 8 *H*–*K*). Overall, our findings suggest that RRx-001 exhibits a potential synergistic effect with ivosidenib in the treatment of IDH1-mutant glioma.

Taken together, we demonstrate that NSUN5, which is epigenetically suppressed by DNA methylation in gliomas, is capable of introducing m5C modification on CTNNB1 caRNA. Meanwhile, NSUN5 induces chromatin recruitment of TET2 and RBFOX2. The m5C modification on caRNA is subsequently converted to 5hmC by TET2, leading to its degradation through recognition by the 5hmC-specific reader RBFOX2. This results in a reduction in the transcription of CD47, tipping the balance in favor of "eat" in the "Don't eat me" signaling pathway. Combination of small molecules RRx-001 and ivosidenib synergistically inhibits glioma growth in vivo by targeting CD47/SIRPα and activation of NSUN5, respectively (Fig. 8*L*).

Discussion

Malignant glioma exhibits extremely immune evasion. Herein, our research has unveiled the critical role played by NSUN5 in modulating glioma immune microenvironment. NSUN5 sequentially induces modifications of m5C and 5hmC on CTNNB1 caRNA to promote its degradation with the aid of TET2 and RBFOX2, thereby blocking the phagocytosis-based immune evasion.

NSUN5 is a highly conserved 28S rRNA m5C methyltransferase in eukaryotes (3). Its role in affecting the assembly of ribosomes leads to reduce the global protein synthesis, and it can also mediate selective translation (15). Additionally, it can interact with RIG-I to recognize extraneous dsRNA (32) and methylate mRNA (4). Our study has identified various substrates of NSUN5, including mRNA, lncRNA, and other ncRNA. NSUN5's regulation of β-catenin level is related to the direct methylation of CTNNB1 caRNA by its highly conserved methyltransferase amino acids cystine 308 and cystine 359 (Fig. 3*B* and *SI Appendix*, Fig. S4*K*), independent of its regulation of ribosome function (Fig. 3 *H* and *I* and *SI Appendix*, Fig. S5 *G* and *H*). We performed site-specific

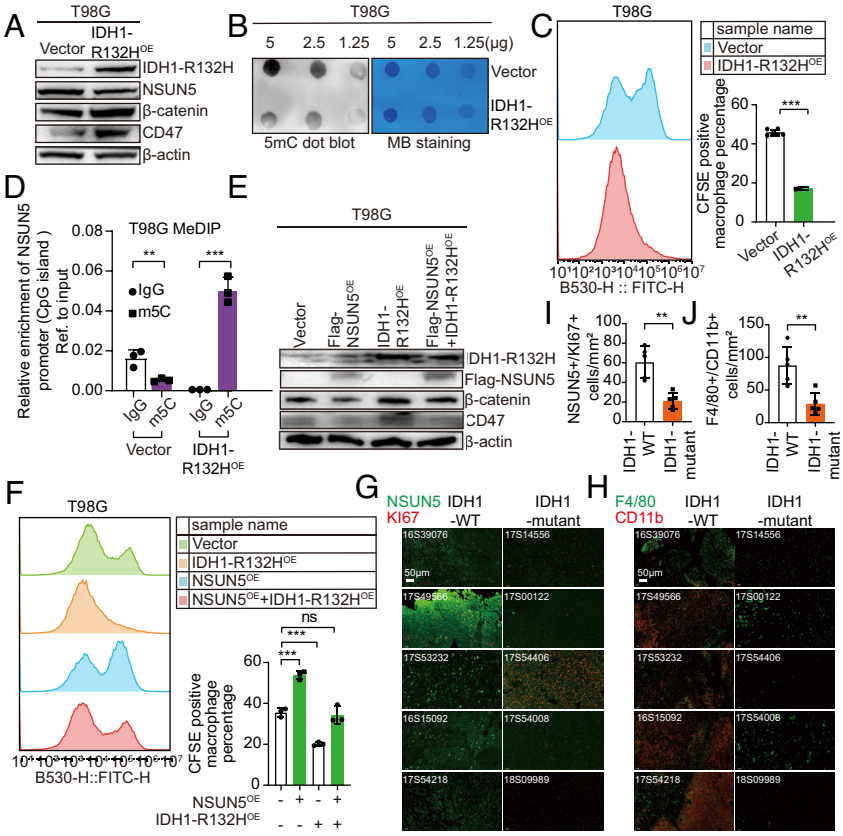

Fig. 7. The IDH1-R132H mutation down-regulates NSUN5 by affecting its genomic methylation in IDH1 mutant gliomas. (*A*) Effects of IDH1-R132H mutation on the NSUN5, β-catenin, and CD47 protein expressions were detected in T98G cells. (*B*) m5C dot blot assay. (*C*) Flow cytometry intensity analysis of fluorescence in macrophages after phagocytosis of CFSE-labeled tumor cells in coculture experiment. The histogram shows the ratio of CFSE-positive macrophages in the coculture experiment. (*D*) The relative enrichment of NSUN5 promoter (CpG island) pulled down by anti-m5C antibody. (*E*) The β-catenin and CD47 protein levels were detected. (*F*) Flow cytometry intensity analysis of fluorescence in macrophages after phagocytosis of CFSE-labeled tumor cells in coculture experiment. The histogram shows the ratio of CFSE-positive macrophages in the coculture experiment. (*G* and *H*) Immunofluorescence analysis showing the expression of NSUN5 and macrophage filtration in glioma patient samples harboring WT or mutant IDH1. (*I* and *J*) For $NSUN5^{+}KI67^{+}$ and $F4/80^{+}CD11b^{+}$ cell counts in immunofluorescence analysis, data were collected from a random field for each patient sample. Data represent mean ± SD; "ns" indicates not significant, $^{**}P < 0.01$, and $^{***}P < 0.001$.

mutation on NSUN5's cystine 359, which significantly inhibited the decrease in β-catenin levels. Interestingly, mutation of cystine 308 resulted in a covalent binding between NSUN5 and its substrate RNA, which was so strong that it directly incapacitated the substrate RNA, causing the same effect as WT NSUN5. To determine the specific nucleic acid sequence recognized by NSUN5, we covalently bound NSUN5 to its target site using the cytidine analog 5-azacytidine and conducted Aza-IP-seq. This led us to identify the site of modification on CTNNB1 mRNA.

It is widely accepted that the same mRNA modification can be recognized by different molecules, leading to different, even opposite outcomes, as seen with the m6A modification (33). The m5C modification on mRNA can enhance mRNA stability through readers such as YBX1 (34) and LIN28B (35), as well as promote nuclear export via the reader ALYREF (36). However, no reader has been identified to induce the degradation of m5C-modified mRNA. Recently, it was reported that NSUN2-mediated m5C modification enhanced the stability of CTNNB1 mRNA (37). Surprisingly, our findings have demonstrated that NSUN5 is involved in the degradation of CTNNB1 caRNA, with this biological process being linked to the sequential modification of 5hmC, which is mediated by TET2. TET2 is a member of the Ten Eleven Translocation (TET) family of enzymes (34). Unlike other members, TET2 lacks the CXXC domain that participates in binding to methylated DNA CpG island (8), which gives it greater flexibility in intracellular localization and substrate binding, allowing it to mediate the hydroxymethylation in RNA (5). We have demonstrated TET2 is capable of hydroxymethylating CTNNB1 mRNA, leading to its degradation (Fig. 5 *D*–*H* and *SI Appendix*, Fig. S9*H*). We have also noticed reduced accessibility of chromatin in cells that overexpress NSUN5 (*SI Appendix*, Fig. S9 *K* and *L*). This suggests that NSUN5 may facilitate the recruitment of TET2 to chromatin. It's particularly thrilling that NSUN5 can enhance the recruitment of TET2 to chromatin, even in the absence of its methyltransferase activity (Fig. 5 *O* and *P*). All of these findings suggest that the process of m5C modification on mRNA is dynamic and connected to TET2-mediated degradation of caRNA.

Since the intersection of Aza-IP and mRNA-seq results contains both up-regulated and down-regulated genes, and their distribution is almost evenly divided (Fig. 4*B*), our study mainly explains why those genes are down-regulated. We are also intrigued by how the up-regulated genes were able to evade degradation by TET2. We believe the answer may be related to the distributional characteristics of TET2 on chromatin. We are unsure whether TET2 could directly bind to its target RNAs or whether it depends on other RBPs. This is because a recent publication has shown that only a subset of TET2-mediated 5hmC-modified mRNAs can be detected by TET2-RIP (38).

The modification 5hmC is known to be present at low levels, and its function is not well characterized. In our study, we propose that RBFOX2 is a reader of 5hmC. Similar to TET2, RBFOX2 has the ability to bind to nascent RNA and inhibit transcription by recruiting Polycomb Complex 2, leading to H3K27me3 modification (11). Notably, a recent study shows that RBFOX2 as a reader capable of

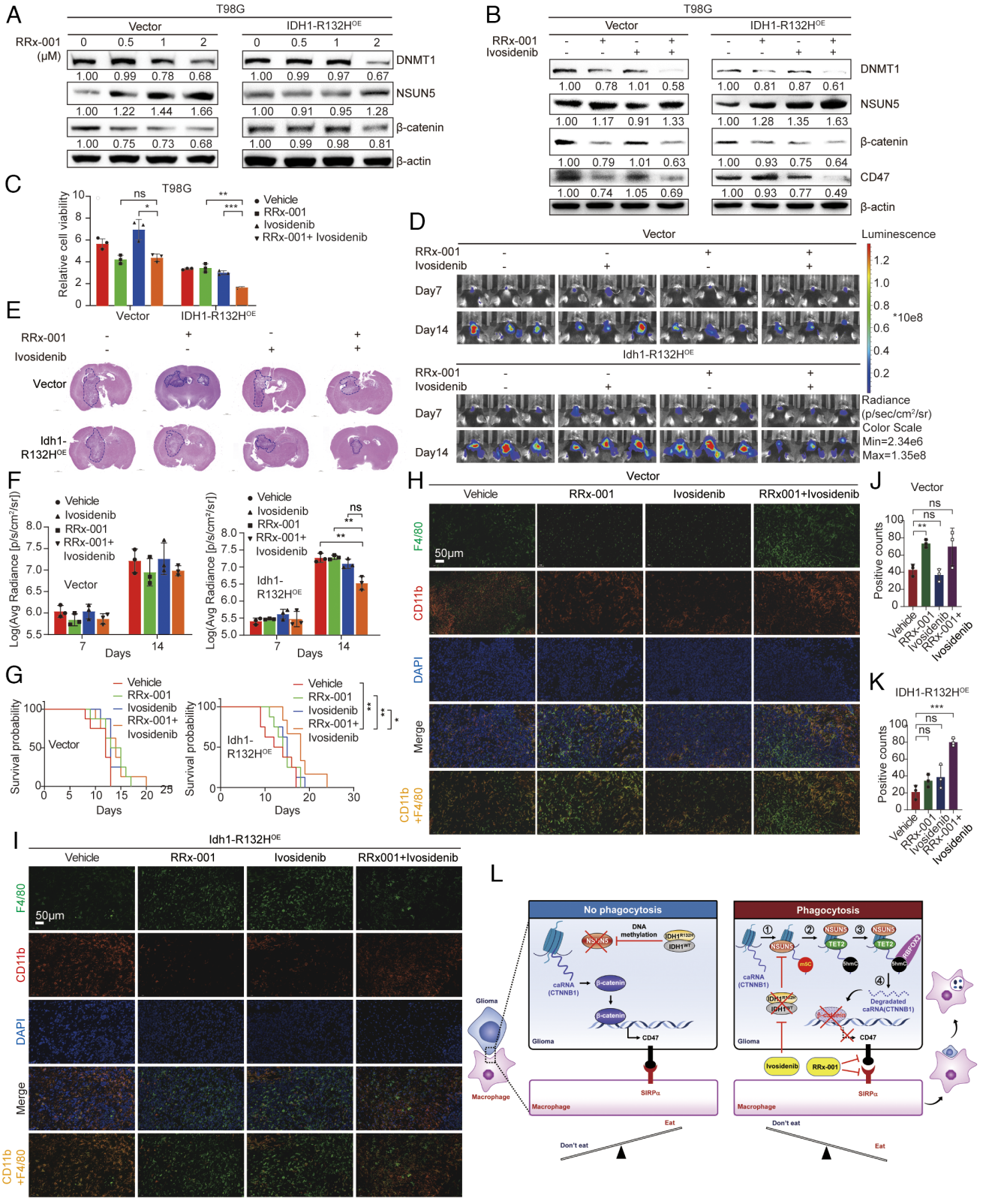

Fig. 8. RRx-001 enhances the antitumor effect of ivosidenib in IDH1 mutant gliomas. (*A* and *B*) The protein levels of DNMT1, NSUN5, CD47, and β-catenin were evaluated and quantified in T98G cells with indicated treatments for 48 h. (*C*) The relative cell viability was measured. Cells were treated with 2 μM RRx001 and/or 5 μM ivosidenib. (*D*) Representative images of luciferase signals from C57BL/6 mice. (*E*) HE staining analysis of the tumor volume at day 10 after implantation from C57BL/6 mice. The tumor size was labeled with dash line. (*F*) Quantification of luciferase activity in panel (*D*). (*G*) Kaplan–Meier analysis was performed to evaluate survival. (*H* and *I*) Immunofluorescence analysis was conducted to assess the infiltration of macrophages represented by CD11b and F4/80 staining at day 13 after implantation from C57BL/6 mice. (*J* and *K*) For F4/80^{+}CD11b^{+} cell counts in immunofluorescence analysis, data were collected from three random fields for each region per mouse. (*L*) Model of NSUN5's role in CTNNB1 caRNA degradation and TAM-mediated phagocytosis of glioma cells. Data represent mean ± SD; "ns" indicates not significant, *P < 0.05, **P < 0.01, and ***P < 0.001.

recognizing m6A modifications on caRNA (39). Our results demonstrate that 5hmC modifications introduced by NSUN5 and TET2 can enhance the binding of RBFOX2 to caRNA/nascent RNA and facilitate the degradation of the target caRNA. This function of RBFOX2 synergistically complements its previously reported role in transcriptional regulation. Additionally, RBFOX2 is a well-known splicing factor involved in alternative splicing, which can influence the stability of its target pre-mRNA (40). Interestingly, we observed that 5hmC was not detected on mature mRNA molecules with polyA tails, suggesting that premature mRNAs with 5hmC undergo extensive degradation. We propose that RBFOX2 may also contribute to abnormal alternative splicing events, ultimately leading to the destabilization of caRNA molecules with 5hmC modifications. Taken together, these findings suggest that RBFOX2 may function as a multifunctional protein, orchestrating its interactions with multiple targets.

Immune therapy has been considered a breakthrough in the treatment of cancer. However, it has been largely unsuccessful in glioma clinical trials. One of the main reasons for this is that glioma is considered a "cold tumor," lacking immune cells in its microenvironment, especially the LGG (41). Therefore, it is crucial to find ways to transform it into a "warm tumor." Our results show that the low expression level of NSUN5 is associated with IDH1 mutation (*SI Appendix*, Fig. S11*A*). The same phenomenon is observed in the glioma patient sample (Fig. 7 *G–J*). We suspect that this could be the reason why IDH1 mutant glioma cells exhibit greater capacity to evade the immune system (42), as well as why patients with IDH1-mutated glioma demonstrate higher resistance to immune therapy (43). Using MeDIP, we identify that IDH1-R132H mutation induces high methylation of the CpG island within the NSUN5 gene promoter (Fig. 7*D*). Restoring NSUN5 in the IDH1-R132H mutant glioma cell could significantly enhance macrophage phagocytosis (Fig. 7 *E* and *F*). In addition, combining the IDH1-R132H inhibitor ivosidenib with RRx-001 could synergistically increase the survival rate and reduce tumor volume (Fig. 8 *D–G*). These results lead us to identify NSUN5 as a critical factor that mediates immune evasion in IDH1 mutant glioma patients. Targeting NSUN5 for macrophage immune therapy, as well as IDH1 mutation, could lead to impressive therapeutic outcomes.

Although m5C is a prevalent and critical modification, its mechanism and regulation have yet to be fully elucidated. One of the most intriguing findings is that previous studies on TET2 and 5hmC in mRNA have mainly concentrated on their destabilizing effects, disregarding the fact that m5C, from which 5hmC is converted, is an important mRNA stabilizer. Our study resolved this paradox by revealing that NSUN5 can recruit TET2 to the chromatin, causing the degradation of the caRNA prior to its maturation and capture by other readers. Although we are unsure of the direct mechanism of recruitment at this moment, data from mass spectrometry analysis suggests that NSUN5 may interact with TAF15, a component of paraspeckles (44) (Dataset S3). It is demonstrated that TET2 can bind to PSPC1 (5) and may play a pivotal role in RNA metabolism within paraspeckles. Interestingly, we observed that NSUN5 localizes in paraspeckles (*SI Appendix*, Fig. S9*J*). Therefore, we propose that dynamic sequential modifications of NSUN5 and TET2 toward CTNNB1 (β-catenin) caRNA may occur in paraspeckles, which warrants further investigation. Overall, our study provides a valuable resource for deciphering the potential biological significance of 5hmC and opens up unique functions for 5hmC modification in caRNA metabolism.

Materials and Methods

Lentivirus Package. For lentivirus production, 293T cells were cultured in 10 cm dishes, and when the cells were 60% confluent, they were transfected with the target plasmid, pMD2g and psPAX2 plasmids. After 48 h of incubation, the packaged virus-containing medium was harvested for subsequent use.

Dot Blot. RNAs were denatured in 65 °C for 15 min and were spotted onto a nylon membrane (GE Healthcare), dried, and cross-linked twice with 120,000 μJ/cm^2 ultraviolet light. The membrane was blocked in 5% BSA in PBS + 0.1% Tween 20 for 1 h before transfer into blocking solution supplemented with 5-mC antibody (Diagenode) and incubated overnight at 4 °C. After secondary antibody incubation and wash, dot blots were visualized using a chemiluminescence ECL kit (Tanon).

Western Blot. Cells were harvested at indicated times, and 30 μg of total protein from each group was used for electrophoresis. The membrane was blocked with 5% nonfat milk at room temperature for 1 h and incubated overnight at 4 °C with primary antibodies against target protein. Subsequently, an anti-rabbit (CST, 7074S) or anti-mouse (CST, 7076S) secondary antibody was applied to the membrane and incubated for 1 h at room temperature. Protein bands were visualized using a chemiluminescence ECL kit (Tanon, Shanghai, China).

Statistical Analysis. The statistical methods used in this study were as follows: Grouped data were expressed as mean ± SD unless otherwise indicated. All in vitro experiments were conducted with a minimum of three replicates. Differences in means between groups were assessed using the two-tailed unpaired Student's *t* test for parametric data or the Mann–Whitney *U* test for nonparametric data when comparing two groups. For comparisons involving multiple groups, one-way ANOVA was utilized. Statistical significance was defined as $P < 0.05$. Survival analysis was performed using Kaplan–Meier survival curves, and differences between groups were evaluated using log-rank statistics. All statistical analyses were conducted using GraphPad Prism 9 software (GraphPad Software, Inc.).

Data, Materials, and Software Availability. The sequencing data generated in this study have been deposited in the SRA repository under accession codes PRJNA1005572 (for RNA-seq), PRJNA995949 (for hmeRIP-seq), and PRJNA998620 (for AzaIP-seq) (45–47). All study data are included in the article and/or supporting information.

ACKNOWLEDGMENTS. We appreciate the technical supports from the Core Facility of Shanghai Medical College, Fudan University, provided by Dr. Lei Zhang and Dr. Xiaoyu Wang, for mass spectrometry analysis. We appreciate Dr. Licheng Zhang for the bioinformation analysis of read density tracks. We would also like to thank Professor Xialian Xu and Dr. Chenyi Rao from Zhongshan Hospital for their generous help. This work was supported by the National Natural Science Foundation of China (Nos. 82073880 and 81872467), the Shanghai Municipal Health Commission (No. 201940233), the Program for Professor of Special Appointment (Eastern Scholar) at Shanghai Institutions of Higher Learning (No. TP2019047), and the Zhengyi Program (S26-13) and Qingfeng Program (QF2209) of Fudan University.

Author affiliations: [a]Department of Pharmacology, School of Basic Medical Sciences, Shanghai Medical College, Fudan University, Shanghai 200032, China; [b]Department of Neurosurgery, Huashan Hospital, Fudan University, Shanghai 200040, China; [c]Department of Neurology, Huashan hospital, Fudan University, Shanghai 200040, China; [d]Department of Endocrinology and Metabolism, Zhongshan Hospital, Fudan University, Shanghai 200032, China; [e]Department of Microbiology, Key Laboratory of Medical Molecular Virology (Ministry of Education/ National Health Commission/ Chinese Academy of Medical Sciences), Shanghai Frontiers Science Center of Pathogenic Microorganisms and Infection, School of Basic Medical Sciences, Shanghai Medical College, Fudan University, Shanghai 200032, China; [f]Department of Pathology, Zhongshan hospital, Fudan University, Shanghai 200032, China; and [g]Department of Logistics, Dalian No.3 People's hospital Affiliated to Dalian Medical University, Dalian 116033, China

Author contributions: M.S. designed research; R.W., C.S., X.C., R. Yang, and H.W. performed research; R.L., Y.H., W.D., B.P., S.F., J.W., F.C., and C.Y. contributed new reagents/analytic tools; R.W., C.S., X.C., R. Yang, Y. Luan, P.Y., R.T., S.B., Y. Li, Y.D., Q.L., Z.F., R. Yan, H.D., and M.S. analyzed data; and R.W., C.S., R. Yang, and M.S. wrote the paper.

1. W. A. Cantara *et al.*, The RNA modification database, RNAMDB: 2011 update. *Nucleic Acids Res.* **39**, D195–201 (2011).
2. J. Ma *et al.*, m5C-Atlas: A comprehensive database for decoding and annotating the 5-methylcytosine (m5C) epitranscriptome. *Nucleic Acids Res.* **50**, D196–D203 (2022).
3. M. Schosserer *et al.*, Methylation of ribosomal RNA by NSUN5 is a conserved mechanism modulating organismal lifespan. *Nat. Commun.* **6**, 6158 (2015).
4. J. Liu *et al.*, The NSUN5-FTH1/FTL pathway mediates ferroptosis in bone marrow-derived mesenchymal stem cells. *Cell Death Discov.* **8**, 99 (2022).

5. D. Guallar *et al.*, RNA-dependent chromatin targeting of TET2 for endogenous retrovirus control in pluripotent stem cells. *Nat. Genet.* **50**, 443–451 (2018).
6. R. A. Morantz, G. W. Wood, M. Foster, M. Clark, K. Gollahon, Macrophages in experimental and human brain tumors. Part 2: Studies of the macrophage content of human brain tumors. *J. Neurosurg.* **50**, 305–311 (1979).
7. J. M. Brown, L. Recht, S. Strober, The promise of targeting macrophages in cancer therapy. *Clin. Cancer Res.* **23**, 3241–3250 (2017).
8. S. Turcan *et al.*, IDH1 mutation is sufficient to establish the glioma hypermethylator phenotype. *Nature* **483**, 479–483 (2012).
9. J. G. Underwood, P. L. Boutz, J. D. Dougherty, P. Stoilov, D. L. Black, Homologues of the Caenorhabditis elegans Fox-1 protein are neuronal splicing regulators in mammals. *Mol. Cell Biol.* **25**, 10005–10016 (2005).
10. J. H. Kim *et al.*, SON drives oncogenic RNA splicing in glioblastoma by regulating PTBP1/PTBP2 switching and RBFOX2 activity. *Nat. Commun.* **12**, 5551 (2021).
11. C. Wei *et al.*, RBFox2 binds nascent RNA to globally regulate polycomb complex 2 targeting in mammalian genomes. *Mol. Cell* **62**, 875–889 (2016).
12. N. Zhang *et al.*, FoxM1 promotes beta-catenin nuclear localization and controls Wnt target-gene expression and glioma tumorigenesis. *Cancer Cell* **20**, 427–442 (2011).
13. A. Veillette, J. Chen, SIRPalpha-CD47 immune checkpoint blockade in anticancer therapy. *Trends Immunol.* **39**, 173–184 (2018).
14. P. Gowda, S. Patrick, A. Singh, T. Sheikh, E. Sen, Mutant isocitrate dehydrogenase 1 disrupts PKM2-beta-catenin-BRG1 transcriptional network-driven CD47 expression. *Mol. Cell Biol.* **38**, e00001-18 (2018).
15. M. Janin *et al.*, Epigenetic loss of RNA-methyltransferase NSUN5 in glioma targets ribosomes to drive a stress adaptive translational program. *Acta Neuropathol.* **138**, 1053–1074 (2019).
16. J. X. Cheng *et al.*, RNA cytosine methylation and methyltransferases mediate chromatin organization and 5-azacytidine response and resistance in leukaemia. *Nat. Commun.* **9**, 1163 (2018).
17. B. Oronsky *et al.*, Rockets, radiosensitizers, and RRx-001: An origin story part I. *Discov. Med.* **21**, 173–180 (2016).
18. B. Oronsky *et al.*, RRx-001, a downregulator of the CD47- SIRPalpha checkpoint pathway, does not cause anemia or thrombocytopenia. *Expert Opin. Drug Metab. Toxicol.* **17**, 355–357 (2021).
19. K. E. Bohnsack, C. Hobartner, M. T. Bohnsack, Eukaryotic 5-methylcytosine (m(5)C) RNA methyltransferases: Mechanisms, cellular functions, and links to disease. *Genes (Basel)* **10**, 102 (2019).
20. G. Yang *et al.*, Poly(ADP-ribosyl)ation mediates early phase histone eviction at DNA lesions. *Nucleic Acids Res.* **48**, 3001–3013 (2020).
21. C. Heissenberger *et al.*, Loss of the ribosomal RNA methyltransferase NSUN5 impairs global protein synthesis and normal growth. *Nucleic Acids Res.* **47**, 11807–11825 (2019).
22. K. D. Rasmussen, K. Helin, Role of TET enzymes in DNA methylation, development, and cancer. *Genes Dev.* **30**, 733–750 (2016).
23. L. Hu *et al.*, Crystal structure of TET2-DNA complex: Insight into TET-mediated 5mC oxidation. *Cell* **155**, 1545–1555 (2013).
24. S. Nakagawa, T. Hirose, Paraspeckle nuclear bodies–useful uselessness? *Cell Mol. Life Sci.* **69**, 3027–3036 (2012).
25. A. Jbara *et al.*, RBFOX2 modulates a metastatic signature of alternative splicing in pancreatic cancer. *Nature* **617**, 147–153 (2023).
26. R. Sesanto, J. F. Kuehn, D. L. Barber, K. A. White, Low pH facilitates heterodimerization of mutant isocitrate dehydrogenase IDH1-R132H and promotes production of 2-hydroxyglutarate. *Biochemistry* **60**, 1983–1994 (2021).
27. L. Bunse *et al.*, Suppression of antitumor T cell immunity by the oncometabolite (R)-2-hydroxyglutarate. *Nat. Med.* **24**, 1192–1203 (2018).
28. M. Friedrich *et al.*, Tryptophan metabolism drives dynamic immunosuppressive myeloid states in IDH-mutant gliomas. *Nat. Cancer* **2**, 723–740 (2021).
29. N. M. Amankulor *et al.*, Mutant IDH1 regulates the tumor-associated immune system in gliomas. *Genes Dev.* **31**, 774–786 (2017).
30. M. Swaminathan, E. S. Wang, Novel therapies for AML: A round-up for clinicians. *Expert Rev. Clin. Pharmacol.* **13**, 1389–1400 (2020).
31. S. H. Tella, A. Mahipal, An evaluation of ivosidenib for the treatment of IDH1-mutant cholangiocarcinoma. *Expert Opin. Pharmacother.* **23**, 1879–1885 (2022).
32. B. Sun *et al.*, NSUN5 facilitates viral RNA recognition by RIG-I receptor. *J. Immunol.* **205**, 3408–3418 (2020).
33. X. Jiang *et al.*, The role of m6A modification in the biological functions and diseases. *Signal Transduct. Target. Ther.* **6**, 74 (2021).
34. X. Chen *et al.*, 5-methylcytosine promotes pathogenesis of bladder cancer through stabilizing mRNAs. *Nat. Cell Biol.* **21**, 978–990 (2019).
35. J. Su *et al.*, NSUN2-mediated RNA 5-methylcytosine promotes esophageal squamous cell carcinoma progression via LIN28B-dependent GRB2 mRNA stabilization. *Oncogene* **40**, 5814–5828 (2021).
36. X. Yang *et al.*, 5-methylcytosine promotes mRNA export - NSUN2 as the methyltransferase and ALYREF as an m(5)C reader. *Cell Res.* **27**, 606–625 (2017).
37. G. Luo *et al.*, NSUN2-mediated RNA m(5)C modification modulates uveal melanoma cell proliferation and migration. *Epigenetics* **17**, 922–933 (2022).
38. J. Lan *et al.*, Functional role of Tet-mediated RNA hydroxymethylcytosine in mouse ES cells and during differentiation. *Nat. Commun.* **11**, 4956 (2020).
39. X. Dou *et al.*, RBFOX2 recognizes N(6)-methyladenosine to suppress transcription and block myeloid leukaemia differentiation. *Nat. Cell Biol.* **25**, 1359–1368 (2023).
40. S. Prashad, P. P. Gopal, RNA-binding proteins in neurological development and disease. *RNA Biol.* **18**, 972–987 (2021).
41. N. Tong *et al.*, Tumor associated macrophages, as the dominant immune cells, are an indispensable target for immunologically cold tumor-glioma therapy? *Front. Cell Dev. Biol.* **9**, 706286 (2021).
42. X. Deng *et al.*, Development and validation of an IDH1-associated immune prognostic signature for diffuse lower-grade glioma. *Front. Oncol.* **9**, 1310 (2019).
43. A. Lal *et al.*, Concurrent versus individual binding of HuR and AUF1 to common labile target mRNAs. *EMBO J.* **23**, 3092–3102 (2004).
44. E. H. Ernst, J. Nielsen, M. B. Ipsen, P. Villesen, K. Lykke-Hartmann, Transcriptome analysis of long non-coding RNAs and genes encoding paraspeckle proteins during human ovarian follicle development. *Front. Cell Dev. Biol.* **6**, 78 (2018).
45. R. Wu *et al.*, RNA-seq. Sequence Read Archive (SRA) repository, PRJNA1005572. https://www.ncbi.nlm.nih.gov/search/all/?term=PRJNA1005572. Accessed 11 August 2023.
46. R. Wu *et al.*, hmeRIP-seq. Sequence Read Archive (SRA) repository, PRJNA995949. https://www.ncbi.nlm.nih.gov/search/all/?term=PRJNA995949. Accessed 18 July 2023.
47. R. Wu *et al.*, AzaIP-seq. Sequence Read Archive (SRA) repository, PRJNA998620. https://www.ncbi.nlm.nih.gov/search/all/?term=PRJNA998620. Accessed 20 July 2023.